N90-12537

APPLICATION OF SOUND AND TEMPERATURE TO CONTROL BOUNDARY-LAYER TRANSITION

L. Maestrello
NASA Langley Research Center
Hampton, Virginia

P. Parikh
Vigyan Research Associates
Hampton, Virginia

A. Bayliss
Northwestern University
Evanston, Illinois

L. S. Huang
NRC Research Associate
Langley Research Center
Hampton, Virginia

T. D. Bryant
NASA Langley Research Center
Hampton, Virginia

ABSTRACT

The growth and decay of a wave packet convecting in a boundary layer over a concave-convex surface and its active control by localized surface heating are studied numerically using direct computations of the Navier-Stokes equations. The resulting sound radiations are computed using linearized Euler equations with the pressure from the Navier-Stokes solution as a time-dependent boundary condition. It is shown that on the concave portion the amplitude of the wave packet increases and its bandwidth broadens while on the convex portion some of the components in the packet are stabilized. The pressure field decays exponentially away from the surface and then algebraically, exhibiting a decay characteristic of acoustic waves in two dimensions. The far-field acoustic behavior exhibits a super-directivity type of behavior with a beaming downstream. Active control by surface heating is shown to reduce the growth of the wave packet but have little effect on acoustic far field behavior for the cases considered.

Active control by sound emanating from the surface of an airfoil in the vicinity of the leading edge is experimentally investigated. The purpose is to control the separated region at high angles of attack. The results show that injection of sound at shedding frequency of the flow is effective in an increase of lift and reduction of drag.

The objective is to study the growth and decay of a wave packet developing over a concave-convex surface and the resulting acoustic radiations. An engineering application is the flow through a wind tunnel contraction. The concave portion is known to be potentially unstable to upstream disturbances while the convex portion is stabilizing. This instability can be reduced by active surface heating. The intensity of resulting sound may still be sufficient to trigger instability downstream, for example, on a model leading edge.

The experimental part is concentrated on separation control by sound emanating from the surface of an airfoil at high angle of attack. This reduces the extent of the separated region, thus improving performance.

OBJECTIVES

- Drag reduction by active surface heating
- Separation control by sound emanating from the surface

TOPICS OF DISCUSSION

- Numerical
  - Study of instability over a concave-convex surface
  - Active control by surface heating
  - Resulting sound radiation
- Experimental
  - Control of flow separation over an airfoil

APPLICATION

The geometry considered is typical of a wind tunnel contraction. The disturbances entering a wall boundary layer in a contraction may grow due to the unfavorable pressure gradient, a source of sound radiation, resulting in both standing and downstream propagating waves. In addition, a patch of turbulence (or vorticity) convecting through the pressure gradient created by the contraction geometry undergoes a variable rate of strain, thereby generating sound. The perturbed field from the boundary layer as well as from the sources embedded in the inviscid flow interact with the leading edge of the model is a possible source of transition.

This presentation includes a study over only one wall of the contraction with disturbances externally imposed in the boundary layer.

WIND TUNNEL CONTRACTION

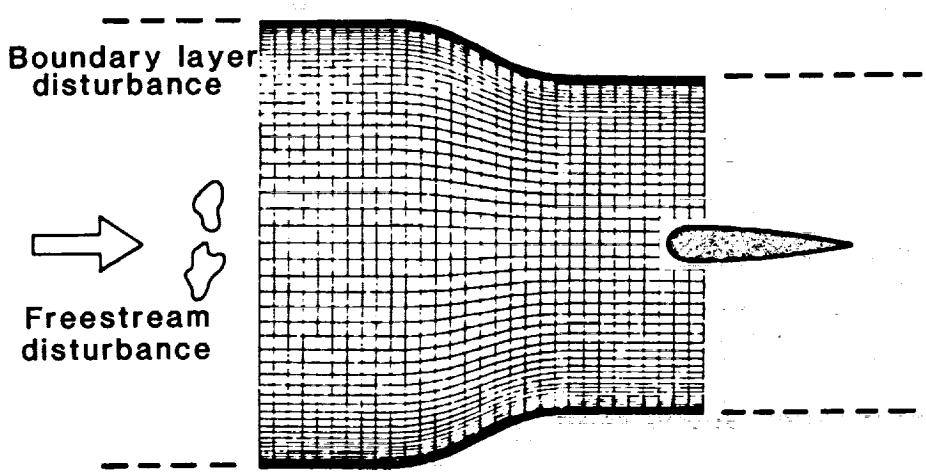

COMPUTATIONAL MODEL

The computations are carried out using two-dimensional laminar, compressible Navier-Stokes equations written in conservation form. The finite-difference scheme used is an explicit predictor-corrector method which is second-order accurate in time and fourth order on convective terms in space. Such an accuracy is needed for reducing numerical dispersion in wave propogation problems.

A steady state is first obtained starting with a boundary-layer solution. An unsteady disturbance in the form of the Orr-Sommerfeld solution is then specified at inflow and an unsteady solution is obtained.

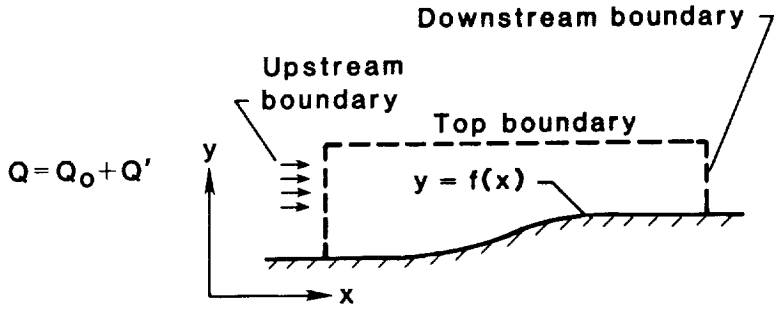

- 2-D Navier-Stokes equations: $W_t+F_x+G_y=0$
  $W=(\rho, \rho u, \rho v, E)^T$
- Predictor-Corrector — F & G are standard flux functions
- Explicit
- 4th Order accurate on convective terms in space
- 2nd Order accurate in time
- Operator splitting
- Q_0 is steady state
  Q' is Orr-Sommerfeld solution

BOUNDARY CONDITIONS

For a complete description, certain boundary conditions must be imposed. At inflow, characteristic boundary conditions are used. Three incoming characteristic variables are obtained from known solutions. In addition, one outgoing characteristic is extrapolated from the interior.

At the top and downstream, radiation boundary conditions are used. This accelerates convergence to steady state and facilitates the upper boundary to be brought closer to the surface.

At the surface, velocities and temperature are specified while the pressure is obtained from normal momentum equation.

- **Inflow**
  - **Specify three incoming characteristics**
    - $p+\rho cu$
    - v
    - $p-\rho c^2$
  - **Extrapolate outgoing characteristic**
    - $p-\rho cu$
- **At top and outer boundaries**
  - **Radiation condition**
    - $p_t - \rho c u_t = 0$ downstream
    - $p_t - \rho c v_t = 0$ top
- **At the wall specify u,v and T**
  Pressure from normal momentum equation

The surface has portions of both concave and convex curvatures. The algebraic equation describing the curve is a seventh-degree polynomial with first three derivatives zero at both ends. This curved surface is accompanied by flat portions both up and downstream. The curve rises to 0.02 ft. in a 1.2-ft. distance. The total length in the streamwise direction is 3.6 ft.

The results presented are for an inflow Mach number of 0.4 and a unit Reynolds number, based on freestream values, of 3.0×10^5. The mean Mach number and pressure distribution are shown. The pressure gradient induced by the surface curvature decelerates the flow at first and then accelerates to a maximum Mach number of about 0.41.

MEAN MACH NUMBER AND PRESSURE DISTRIBUTION

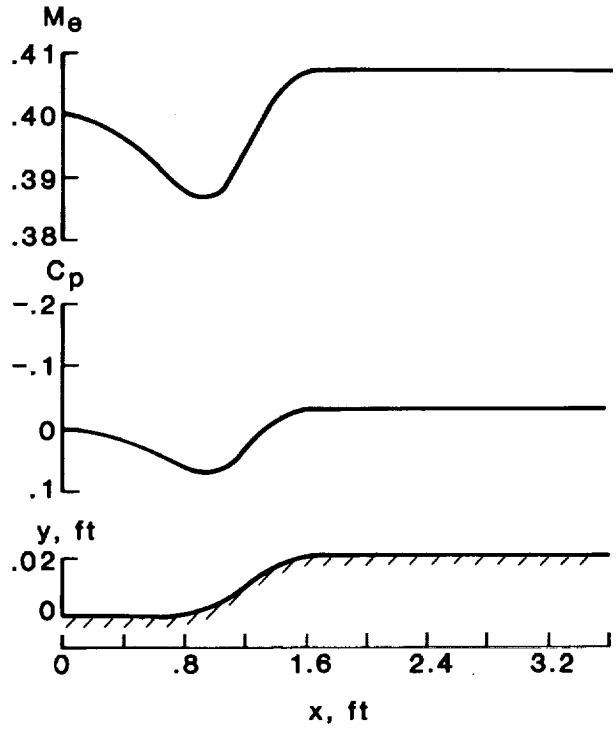

UNSTEADY FLOW - GROWTH OF DISTURBANCES

The unsteady flow is obtained by introducing disturbances (in the form of a wave packet obtained from the Orr-Sommerfeld solution) on the mean flow. The growth of the disturbances is shown in terms of the root mean square (rms) of the massflux integrated across the boundary layer. The value at each station is normalized by the inflow value. The disturbance is initially amplified on the flat portion. Additional amplification comes on the concave curvature due to the unfavorable pressure gradient. Farther downstream, the favorable pressure gradient results in a reduction of growth, followed by an exponential-like growth on the flat portion.

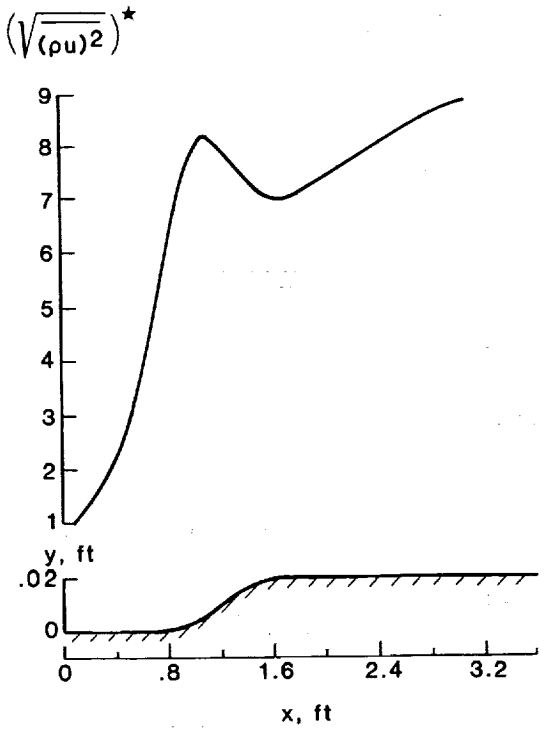

UNSTEADY FLOW - INSTANTANEOUS TOTAL VORTICITY

The instantaneous total vorticity is shown at successive times as the wave packet passes over the surface. The same range of vorticity is plotted for all the frames. The figure distinctively shows that as the disturbance passes over the concave portion, it changes in amplitude and broadens in bandwidth. Further, on the convex portion, drastic changes occur in the bandwidth showing that the favorable pressure gradient stabilizes certain components, as if the flow has passed through a bandpass filter. The phenomenon is strongly dependent upon the geometry of the curvature inducing the pressure gradient.

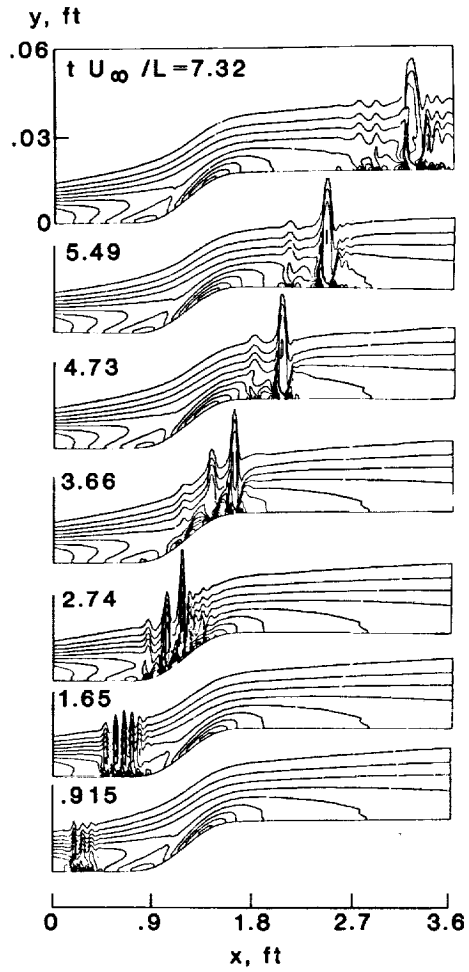

UNSTEADY FLOW - MASS FLUX ALONG THE SURFACE

Further details of the unsteady flow are shown in terms of the mass flux variation with time at several locations along the surface for a fixed distance away from the wall in the boundary layer. It is clear that the initial packet grows both in amplitude and bandwidth over the initial portion and reaches a maximum at x = 1.0 feet, just downstream of the concave portion, thus showing a strong non-linear behavior. This is followed by a significant decay in the favorable pressure gradient portion of the curvature and a growth again on the flat portion downstream.

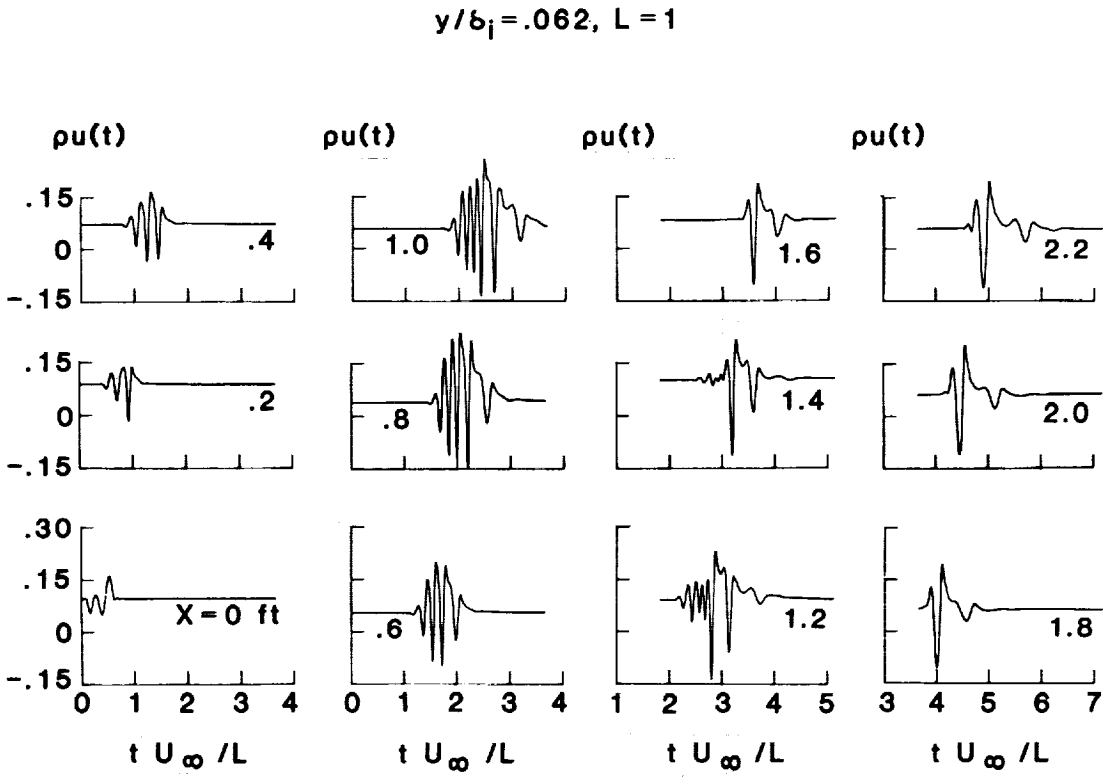

SPACE-TIME GROWTH OF PERTURBATION PRESSURE

This figure shows the space-time variation or the perturbation pressure at a fixed distance away from the wall. The additional information provided by this picture is that the crests of different waves reach their maximum at different positions on the surface indicating stability for some while continuous growth for others. The time rate of change of pressure is responsible for acoustic radiations. A larger height of the surface may further reduce the growth of the disturbances, but a resulting sound field could be larger. In this context, the resulting sound can be viewed as a source of instability.

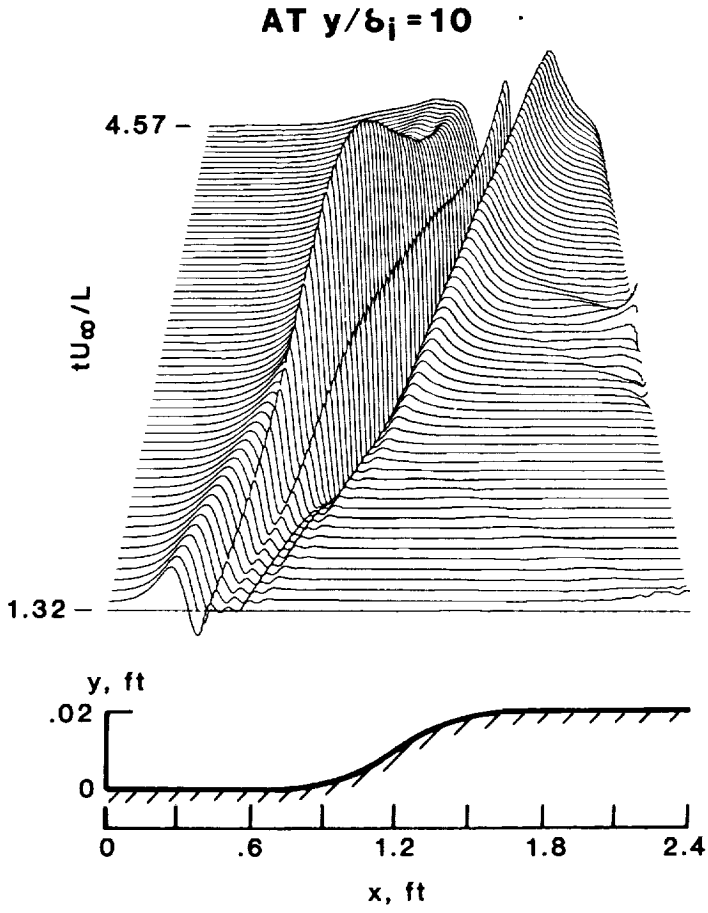

ACTIVE CONTROL - EFFECT ON DISTURBANCE GROWTH

Active control by surface heating is modeled by modifying the temperature boundary condition over a small portion of the surface. The control temperature is applied for a finite time interval coinciding with the passage of the wave packet over the control strip location. The control strip is located in the region of unfavorable pressure gradient at x = 0.9 feet. This location was selected because it is a region of large growth and also because the coupling of the control with the flow is favorable.

The control is not optimized. Larger reductions in growth can be achieved by optimizing amplitude and phase as well as using multiple control strips.

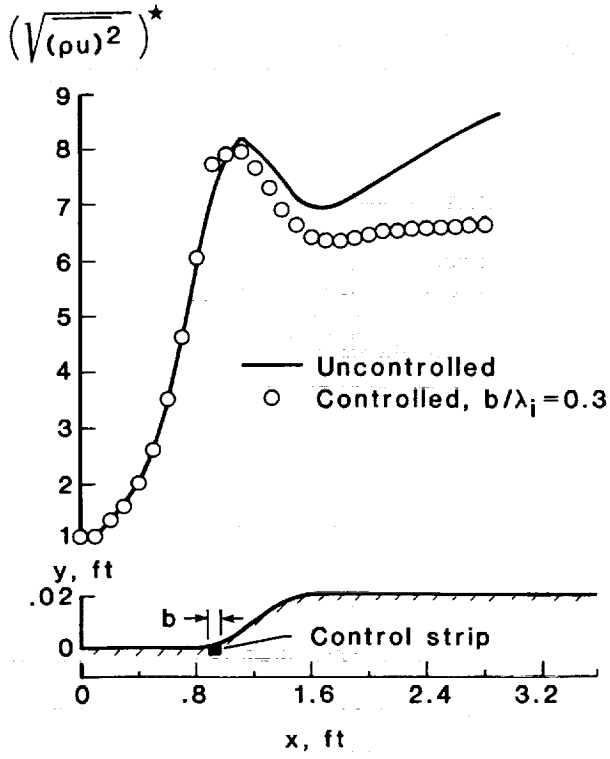

DETERMINATION OF ACOUSTIC FIELD

Due to the vastly different length scales between the acoustic far field and the boundary layer, it is not feasible to compute the acoustic far field concurrently with the Navier-Stokes simulation. The acoustic analogy introduced by Lighthill (ref. 1) provides a formalism to couple wave equations in order to determine the acoustic far field with the near field behavior of the viscous flow. The unsteady near field (generally including turbulent fluctuations) is used as a source term for a convective wave equation describing the far-field acoustic behavior. Our approach is to solve the linearized Euler equations using the pressure computed from the Navier-Stokes solution as a time-dependent boundary condition. We ignore the curvature of the surface because it is considered negligible on the acoustic length scale.

- **Due to vastly different length scales between the acoustic far-field and the boundary layer, it is not feasible to compute acoustics from the Navier-Stokes solution**
- **The acoustic field is evaluated by solving linearized Euler equations using pressure from the N-S as time dependent boundary condition**
- **This approach is an exact instance of the Lighthill's acoustic analogy**

$$p_t + p_x + \frac{(u_x + v_y)}{M^2} = 0$$

$$u_t + u_x + p_x = 0$$

$$v_t + v_x + p_y = 0$$

B.C. $p(x,o,t) \rightarrow$ known from the N-S solution

WALL PRESSURE PERTURBATION ALONG THE SURFACE

The acoustic radiations, which depend on the time rate of changes within the flow, are present even when the flow is being stabilized. In addition, acoustic radiations are known to produce instability leading to transition. Therefore, it is important to study not only the flow instability but the acoustic radiations as well.

The pressure perturbation versus time is shown at different stations along the wall. This is used as an input to the linearized Euler equations to calculate the acoustic field. It may be noticed that the maximum amplitude and bandwidth are around x = 1.0 ft., which is on a location corresponding to maximum growth.

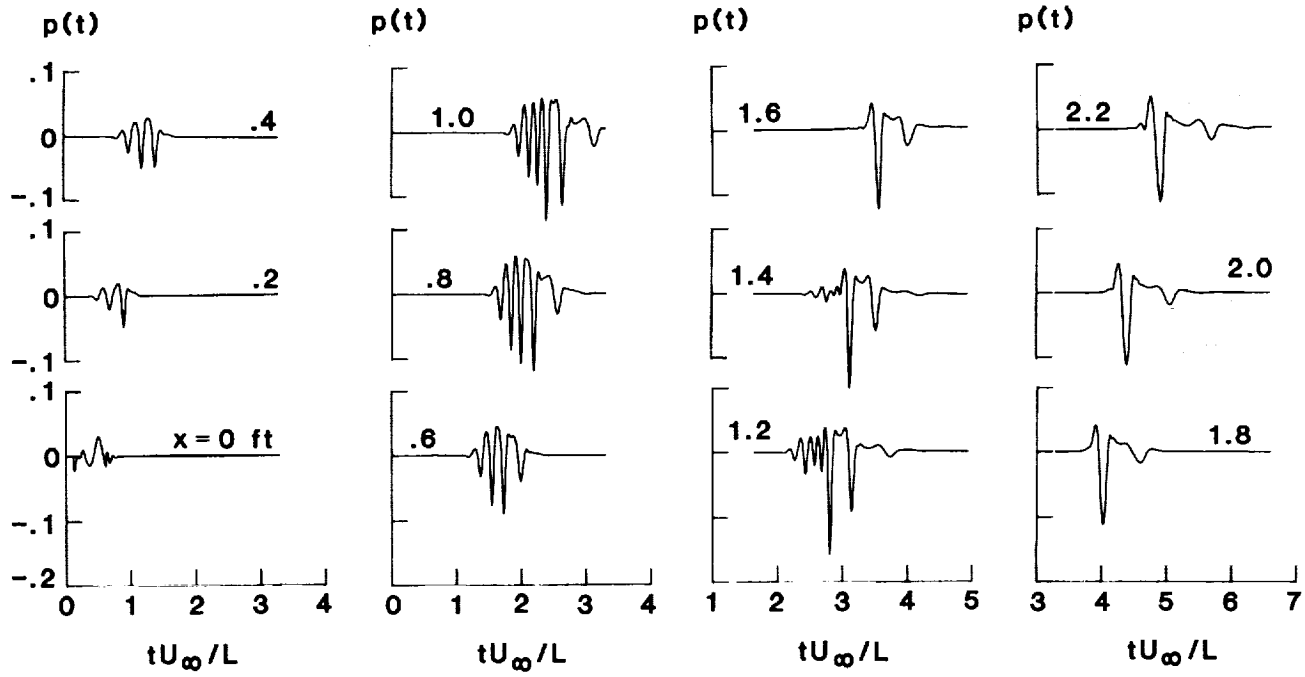

POWER SPECTRA OF WALL PRESSURE PERTURBATIONS

The power spectral density of the wall pressure shows that in addition to the two input frequencies comprising the wave packet, two other frequencies appear between x = 0.8 ft. and 1.2 ft. carrying most of the energy. This is a result of the instability produced by the concave surface. In the convex region and the flat region that follows, the energy content of these two additional modes is reduced drastically and the two original frequencies reappear at x = 1.6 ft.

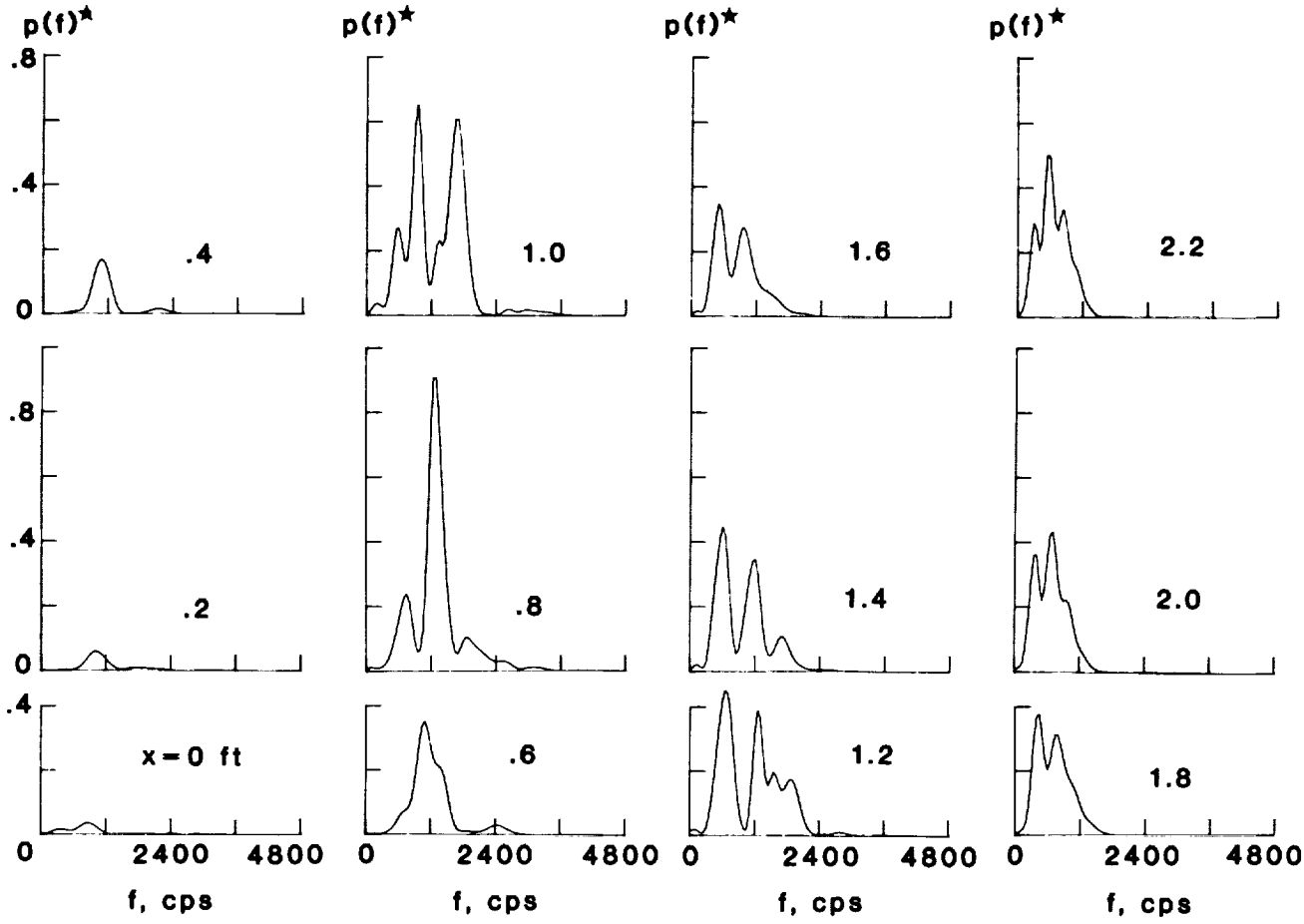

DECAY OF TOTAL POWER WITH DISTANCE FROM THE SURFACE

In order to establish the near- and the far-field behavior, total acoustic power is plotted against the distance from the wall. Two distinct regions can be identified, one close to the boundary (y ~ 5 ft.) where the decay is exponential and the other farther away with an algebraic decay, the acoustic far field.

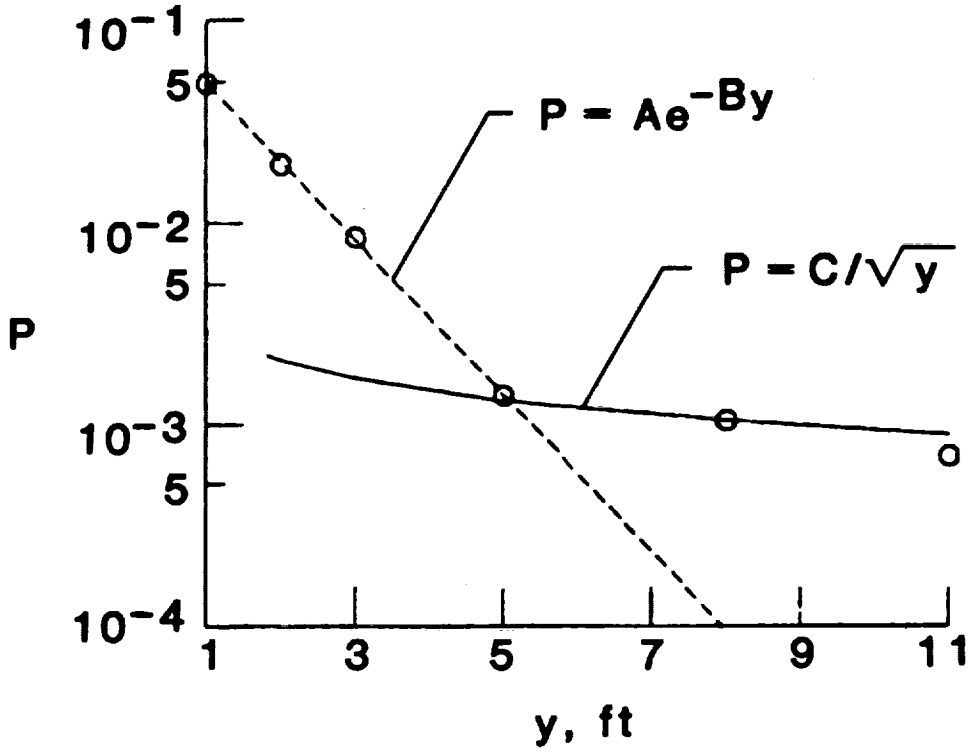

ACOUSTIC PRESSURE AT 11 FT. RADIUS

The acoustic pressure at a radius of 11.0 ft. from the surface is shown at various angular positions between 30° and 150°. Two distinct features are noticeable. One is the sound resulting from the input instability. This reaches the far field at different times due to convection. The other is the sound radiated due to the growth and decay of the wave packet. This component has strong beaming characteristics in the downstream direction. In addition, the modulation resulting from the passage of the wave packet on the curved surface can be clearly seen. Such strong amplitude and directivity have special significance when originating from a wind tunnel contraction since they may trip instability at the model's leading edge.

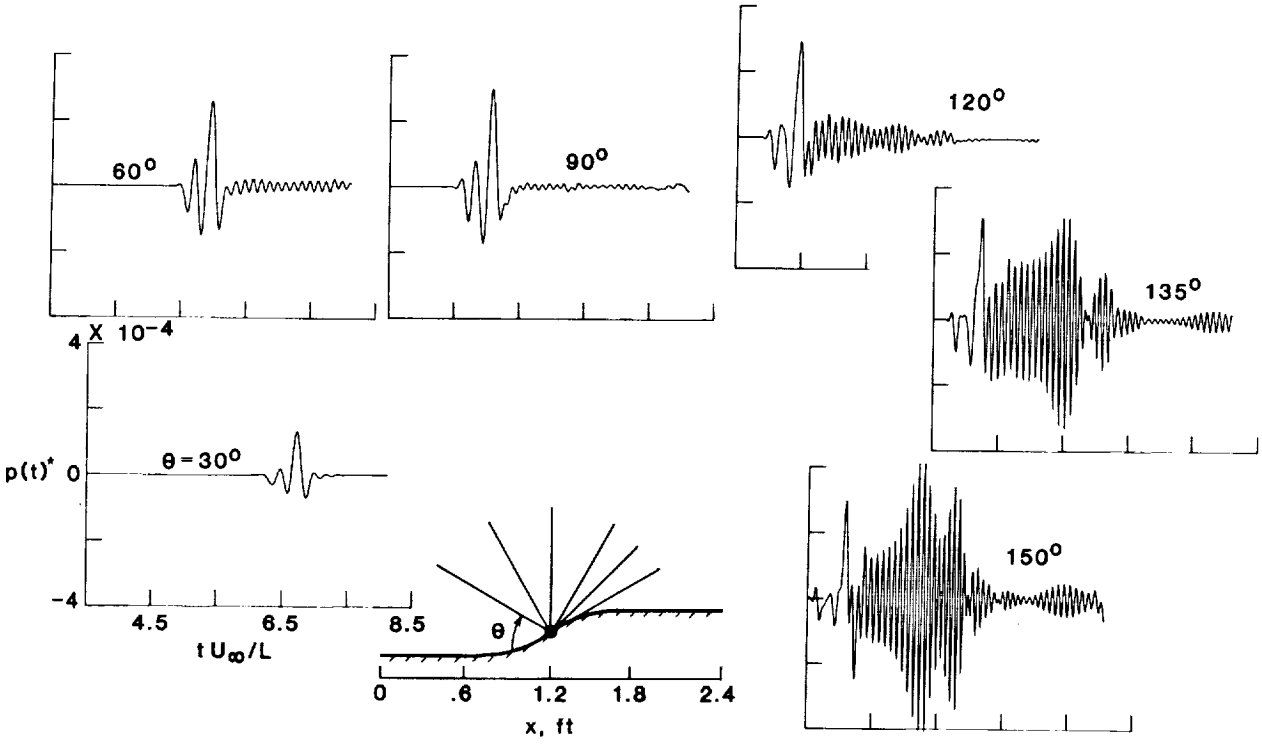

PSD OF ACOUSTIC PRESSURE AT 11 FT. RADIUS

The power spectral density (PSD) of the radiated acoustic field is shown at 11.0 ft. from the surface at various angular positions. Most of the sound is directed downstream with a widening in bandwidth near $\theta = 150°$. The predominant radiation frequencies are those resulting from the growth and decay of the wave packet.

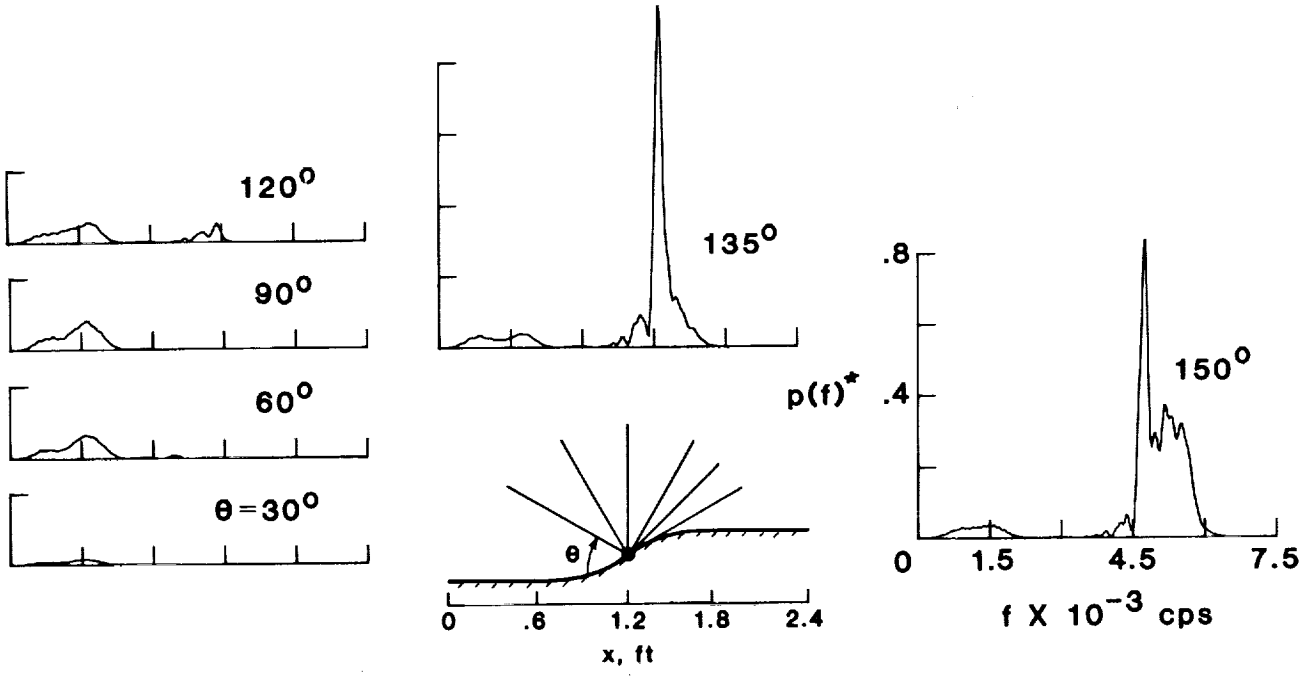

SEPARATION CONTROL BY SOUND OVER AN AIRFOIL

This section concerns an experiment designed to study the effect of sound emanating from the surface of an airfoil on the separated flow at higher angles of attack. At high angles of attack the free shear layer, which sheds from the point of separation, displays the characteristic instability, whereby a sequence of discrete vortex forms. The aim is to study the coupling between the sound and the flow and its effect on separation. This coupling is utilized to increase circulation, stall angle, as well as to reduce the drag of an airfoil.

The experiment was conducted in the 2- by 6-inch wind tunnel at low Reynolds number. Smoke visualization and a hot wire were used to study the flow.

- **Experimental study of the effect of acoustic perturbation on pressure distribution, lift and drag**
- **Shear layer is very sensitive to the excitation field emanating from the surface in the vicinity of the separation**
- **This sensitivity between sound and the local field is used to impart dramatic favorable changes to the flow**

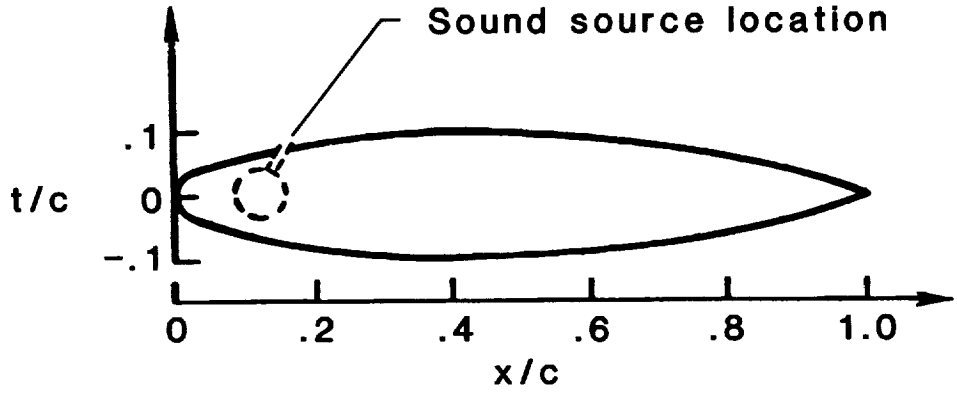

RESULTS - BEHAVIOR OF THE SHEAR LAYER

At high angles, α = 15 and 20 degrees, the flow separates over most of the upper surface. Typical velocity power spectra at different locations over the upper surface of the airfoil are shown (left). At x/c = 0.02, only a low-frequency peak is observed. This peak frequency is approximately 50 Hz and corresponds to the "shedding" frequency of the wake region. Further downstream from the leading edge, x/c = 0.22, other peaks appear with frequencies of 125, 250, and 500 Hz. This observation suggests that the separated shear layer forms and develops with a fundamental frequency of about 500 Hz at a distance away from the leading edge. We notice also that the predominant frequencies in the shear layer vary with the second power of freestream velocity (right figure).

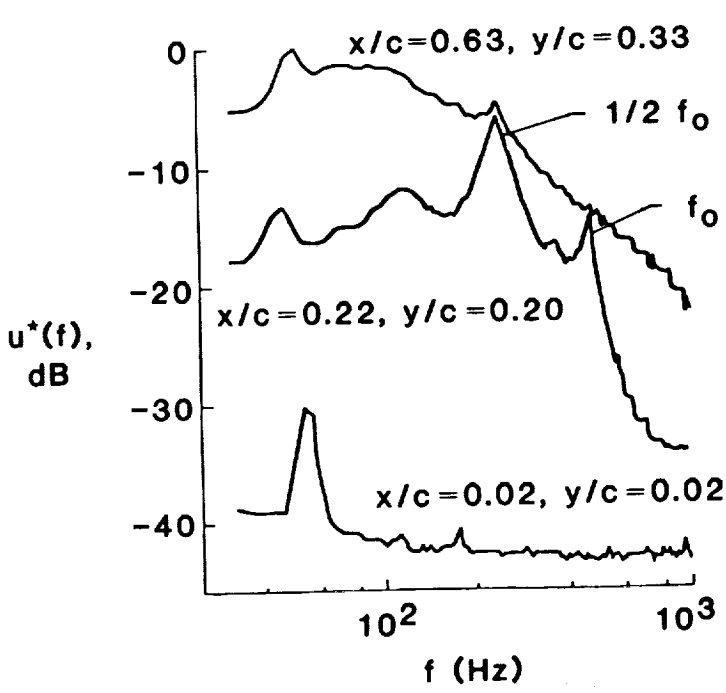

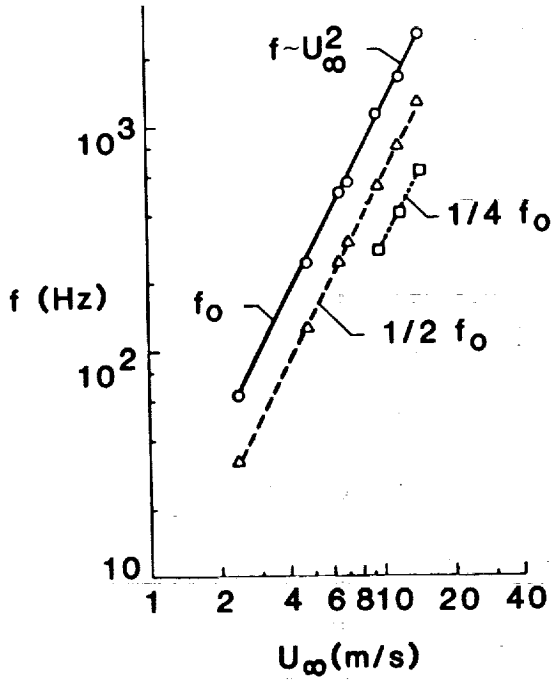

RESULTS - SMOKE VISUALIZATION

A smoke visualization technique is used to see the effectiveness of control by sound. For the uncontrolled case, a large region of separation can be seen on the upper surface. Separation control is achieved by sound injected from a narrow slot located at x/c = 0.15 on the upper surface. When forced exitation at one of the subharmonic frequencies is applied, the separated region becomes drastically reduced. The figure shows the controlled and the uncontrolled pictures.

It is remarkable that a single injection gap can induce such a dramatic change in reducing the area of separation in contrast to the relatively modest control that is achieved at small angles of attack.

$Re_c = 3.5 \times 10^4$, f = 100 Hz

UNCONTROLLED CONTROLLED

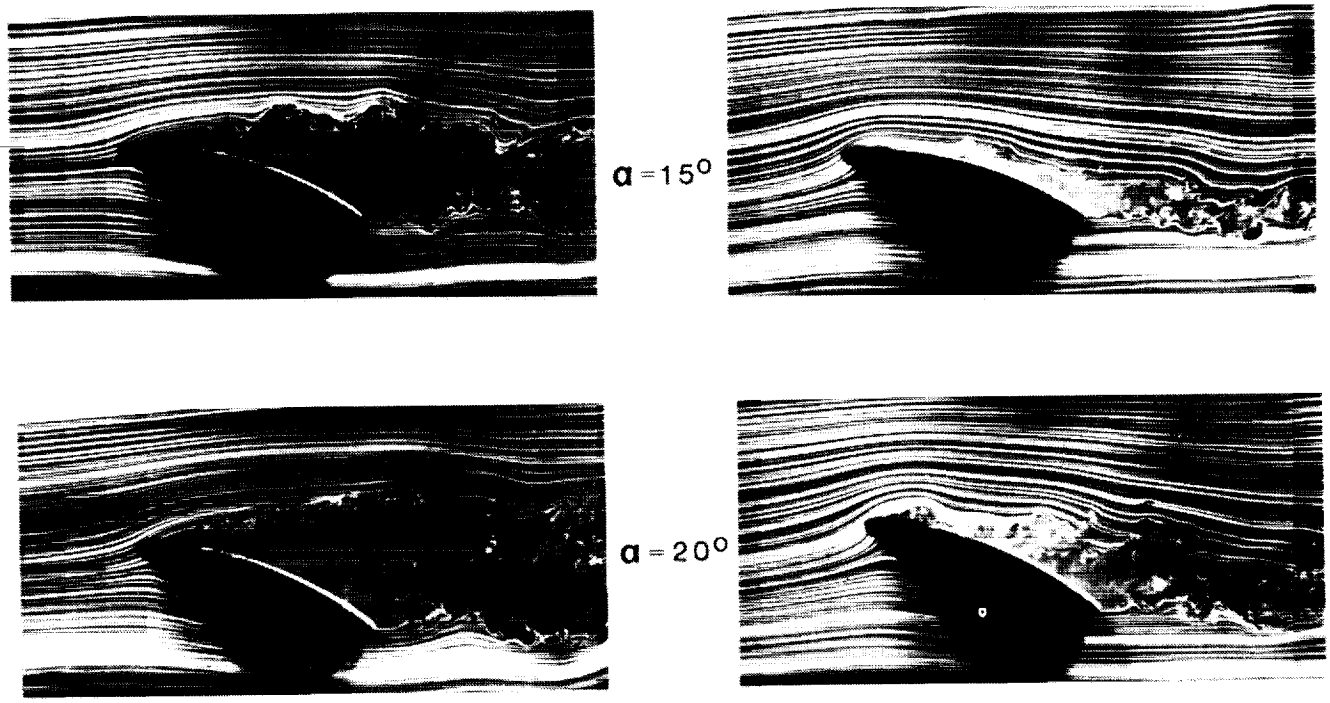

CONTROL OF LIFT AND WAKE PROFILES

The effectiveness of control is plotted in terms of the lift coefficient versus the angle of attack and a typical wake profile at one angle of attack. The gain in lift over the whole range of angle of attack is apparent. Similarly, the defect in the wake profile becomes much smaller, indicating a reduction in drag.

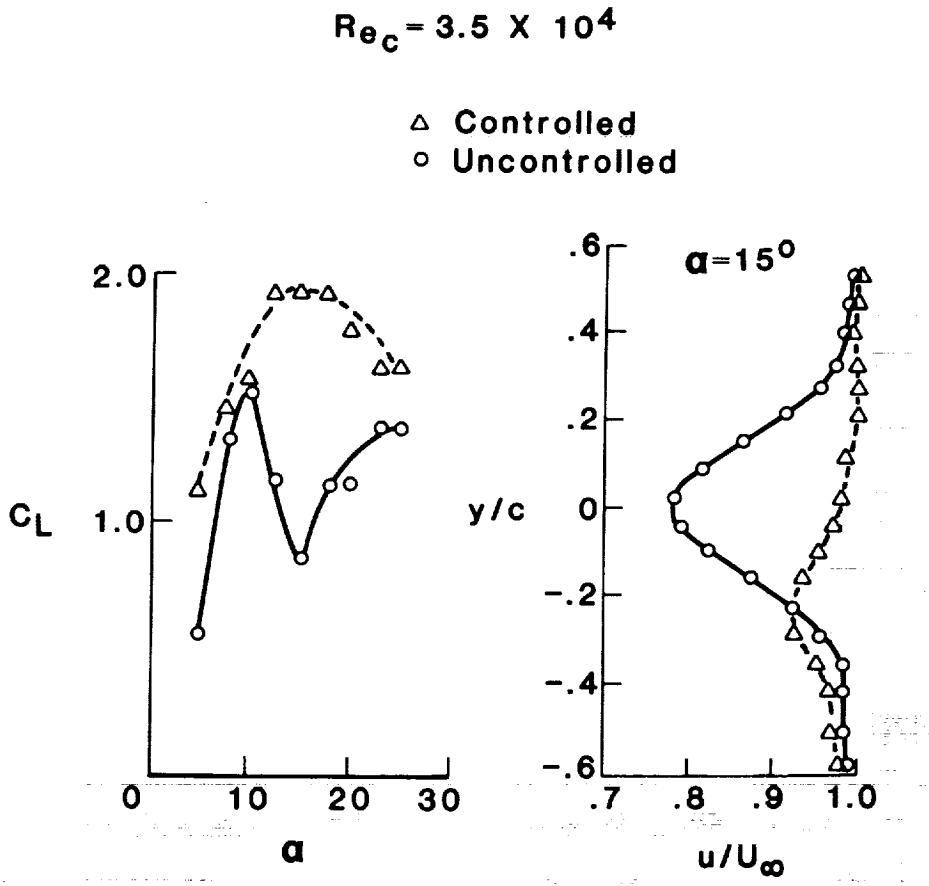

CONCLUDING REMARKS

- Flow control using active surface heating and sound is a powerful and effective technique

BENEFITS

- Development of low drag configurations by control for laminar and turbulent flows
- Optimization of control technique for flows with periodic and random behavior

FUTURE DIRECTIONS

- Extension to turbulent and high speed flows
- Application to realistic aircraft configurations
- Design of wind tunnel contractions with minimum flow and acoustic interference

REFERENCE

1. Lighthill, M. J.: On Sound Generated Aerodynamically. I. General Theory, Proc. Roy Soc. A., 211, 1952, pp. 564-587.